Accepted Manuscript

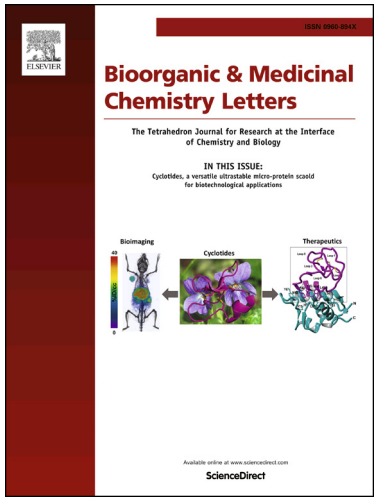

An orally available, brain-penetrant CAMKK2 inhibitor reduces food intake in rodent model

Daniel J. Price, David H. Drewry, Lee T. Schaller, Brian D. Thompson, Paul R. Reid, Patrick R. Maloney, Xi Liang, Periette Banker, Richard G. Buckholz, Paula K. Selley, Octerloney B. McDonald, Jeffery L. Smith, Todd W. Shearer, Richard Cox, Shawn P. Williams, Robert A. Reid, Stefano Tacconi, Federico Faggioni, Chiara Piubelli, Ilaria Sartori, Michela Tessari, Tony Y. Wang

PII: S0960-894X(18)30223-3
DOI: https://doi.org/10.1016/j.bmcl.2018.03.034
Reference: BMCL 25688

To appear in: *Bioorganic & Medicinal Chemistry Letters*

Received Date: 11 December 2017
Revised Date: 12 March 2018
Accepted Date: 13 March 2018

Please cite this article as: Price, D.J., Drewry, D.H., Schaller, L.T., Thompson, B.D., Reid, P.R., Maloney, P.R., Liang, X., Banker, P., Buckholz, R.G., Selley, P.K., McDonald, O.B., Smith, J.L., Shearer, T.W., Cox, R., Williams, S.P., Reid, R.A., Tacconi, S., Faggioni, F., Piubelli, C., Sartori, I., Tessari, M., Wang, T.Y., An orally available, brain-penetrant CAMKK2 inhibitor reduces food intake in rodent model, *Bioorganic & Medicinal Chemistry Letters* (2018), doi: https://doi.org/10.1016/j.bmcl.2018.03.034

Bioorganic & Medicinal Chemistry Letters
journal homepage: www.elsevier.com

An orally available, brain-penetrant CAMKK2 inhibitor reduces food intake in rodent model

Daniel J. Price [a,*], David H. Drewry[b], Lee T. Schaller[a], Brian D. Thompson[b], Paul R. Reid[b], Patrick R. Maloney[b], Xi Liang[b], Periette Banker[a], Richard G. Buckholz[a], Paula K. Selley[b], Octerloney B. McDonald[b], Jeffery L. Smith[b], Todd W. Shearer[b], Richard Cox[b], Shawn P. Williams [a], Robert A. Reid [a], Stefano Tacconi[b], Federico Faggioni[b], Chiara Piubelli[b], Ilaria Sartori[b], Michela Tessari[b], and Tony Y. Wang[b]

[a]*GlaxoSmithKline, 5 Moore Drive, Research Triangle Park, NC 27709, USA*
[b]*All research described was performed as employees of GlaxoSmithKline. Current affiliations supplied in footnote 25.*

ARTICLE INFO

Article history:
Received
Revised
Accepted
Available online

Keywords:
CAMKK2
Inhibitor
Satiety

ABSTRACT

Hypothalamic CAMKK2 represents a potential mechanism for chemically affecting satiety and promoting weight loss in clinically obese patients. Single-digit nanomolar inhibitors of CAMKK2 were identified in three related ATP-competitive series. Limited optimization of kinase selectivity, solubility, and pharmacokinetic properties were undertaken on all three series, as SAR was often transferrable. Ultimately, a 2,4-diaryl 7-azaindole was optimized to afford a tool molecule that potently inhibits AMPK phosphorylation in a hypothalamus-derived cell line, is orally bioavailable, and crosses the blood-brain barrier. When dosed orally in rodents, compound **4t** limited ghrelin-induced food intake.

The detrimental implications of obesity on human health have been well documented,[1] and novel mechanisms for therapeutically promoting weight loss would have significant medical and social benefits. AMPK is a central integrator of hormone and energy sensing in the hypothalamus, controlling satiety via NPY expression. Central AMPK inhibition reduces NPY-mediated feeding, however, peripheral inhibition of AMPK promotes an undesirable anabolic phenotype for obese patients: increased lipogenesis, cholesterol and glycogen synthesis, gluconeogenesis, and a concomitant decrease in processes such as fatty acid oxidation and serum glucose uptake.[2] Intriguingly, LKB1 is recognized as the predominant mediator of AMPK phosphorylation in response to peripheral energy demand,[3-4] whereas CAMKK2 has been identified as the hypothalamic AMPK kinase that transduces Ca++-mediated ghrelin signaling,[5] thus suggesting a mechanism to selectively inhibit hypothalamic AMPK and NPY's downstream orexigenic effect.

Indeed, CAMKK2-null mice show a sustained reduction in feeding on a high-fat diet and have resultingly lower body weights, reduced adiposity, and improved glucose sensitivity relative to their WT littermates.[5] From a mechanistic standpoint, CAMKK2-null mice are acutely resistant to ghrelin-induced food intake, and eat less than their WT counterparts upon refeeding after fasting, similar to NPY-depleted mice.[5] These latter observations are corroborated by pharmacological inhibition of CAMKK2 using STO-609 delivered via i.c.v. administration.[5] CAMKK2's role in other processes and tissues is still being elucidated, however. Whole and tissue-specific knock-out of CAMKK2 have implicated it in glycemic control through a liver-specifc, AMPK-independent mechanism,[6] bone density via osteoblast/osteoclast ratio,[7] and long-term memory formation.[8] We set out to identify an orally available, brain-penetrant CAMKK2 inhibitor to probe the holistic impact of inhibiting CAMKK2 with a therapy-relevant modality, with an immediate goal of further substantiating the therapeutic hypothesis of acutely reducing feeding.

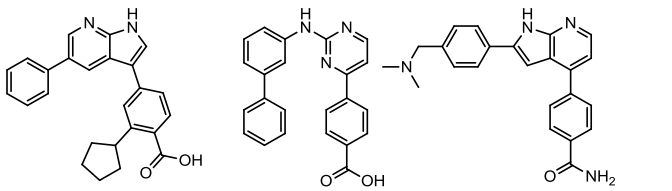

1a, pIC50 CAMKK2 = 9.2 **3a**, pIC50 CAMKK2 = 8.1 **4a**, pIC50 CAMKK2 = 8.5

Figure 1. Three hits identified in focused screen.

A fluorescent polarization-based assay of full length CAMKK2 was established for primary screening.[9] A screen of ~12K compounds focused on known ATP-competitive kinase

inhibitors and compounds with pharmacophoric features similar to known kinase inhibitors identified several potent starting points for a chemistry campaign (Figure 1). Potent inhibitors were subsequently advanced to an ELISA-based assay monitoring AMPK phosphorylation in the catalytic alpha subunit at Thr172 in the mouse neuronal N39 cell line to measure CAMKK2 activity in a hypothalamus-relevant cell model.[10] Biochemical ortholog assays were deemed unnecessary based on sequence identity.[11]

Our leads suggested high CAMKK2 potency is achievable, though several properties would need to be optimized. Each of the leads has been screened against 48-86 other kinases in dose response, and is active on 15-30% of those with an IC50 <100 nM. Selectivity for CAMKK2 therefore required optimization, which is perhaps not surprising as each template largely conforms to a published generic pharmacophore for kinase inhibition.[12] As a correlation has been established relating increasing aromaticity to poor solubility,[13] we aimed to monitor and optimize solubility using a high-throughput assay.[14] Finally, the properties of brain-penetrant molecules have also been well described,[15] and while some calculated properties of the 3 leads (e.g. $66 \leq$ tpsa ≤ 75, $367 \leq$ mw ≤ 382, # hbond donors ≤ 2)[16] are similar to those seen in retrospective analyses of CNS-active drugs, the benzoic acid of **1a** and **3a** is likely incompatible with CNS exposure.

We expected from initial modeling that the 2-amino pyrimidine of **3a** and 7-azaindoles of **1a** and **4a** would bind the so-called kinase hinge, albeit the latter two doing so in an opposite orientation relative to each other. Furthermore, it was anticipated that the benzoic acid of **1a** and **3a** and benzamide of **4a** would interact directly with the catalytic lysine. The pharmacophoric similarity of the molecules suggested that the SAR would be transferable across series, and in particular that the benzamide would be a suitable replacement for the benzoic acid. We therefore pursued concerted optimization of the three series together.

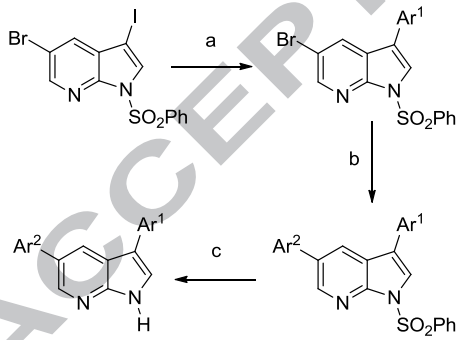

Scheme 1. Reagents and conditions: (a) 1 eq $Ar^1B(OH)_2$, 0.064 eq $Pd(dppf)Cl_2$, 5.24 eq Na_2CO_3 in 1,4-dioxane, reflux, 105 °C, 3 days, (b) 2 eq $Ar^2B(OH)_2$, 4.68 eq Na_2CO_3, 0.115 eq $PdCl_2$ in 1,4-dioxane, 15 hrs, 100 °C, (c) 3 eq K_2CO_3 in MeOH, 50 °C, 65 hrs.

Synthesis of 3,5-diaryl 7-azaindoles from commercially available starting materials has been previously described[17]; related conditions and reagents used here afforded rapid SAR expansion (Scheme 1). A strong dependency for larger alkanes *ortho*- to the benzoic acid was quickly identified (**1a**-**1f** in Table 1), a feature we hoped would benefit the other templates. While placing a greasy group under the G-rich loop might appear to be a promiscuous feature and increase potency on all kinases, we found that larger substituents at this position and/or the induced rotation of the acid were neutral or detrimental to the activity against many other kinases screened. For example, the unsubstituted benzoic acid (**1f**) is roughly equipotent on CAMKK2 and CK2 whereas the cyclopentyl benzoic acid (**1a**) displays 1000x selectivity for CAMKK2 over CK2 (CK2 data not shown). Unfortunately, the acids had poor cellular activity (IC50 >1 μM), perhaps reflecting poor cellular penetration.

Matched pairs from the initial screen suggested several acid replacements (alcohol, methyl ether, ethyl sulfone, and N-linked methyl sulfonamide) are poorly tolerated. Homologation of the acid by one or two carbons is detrimental as well (data not shown). The benzamide was confirmed as near equipotent with the unsubstituted benzoic acid (**1i**-**1l**) as is the acid isostere tetrazole **1g**, whereas the methyl ester **1h** showed reduced potency. Unfortunately, substitution of an alkane adjacent to the benzamide did not boost potency like with the acids (e.g. **1j** vs **1p**).

Table 1. 3,5-diaryl 7-azaindoles.

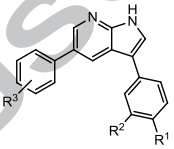

	R^1	R^2	R^3	Sol[a] (μM)	CAMKK2 pIC50	P-AMPK pIC50
1a	COOH	cyclopentyl	H	150	9.2	5.9
1b	COOH	isobutyl	H	333	8.3	
1c	COOH	isopropyl	H	>439	8.4	5.9
1d	COOH	CH_2CH_3	H	178	7.7	
1e	COOH	CH_3	H	100	7.3	
1f	COOH	H	H	82	6.7	
1g	tetrazole	H	H	276	6.4	
1h	CO_2Me	H	H	5	5.9	
1i	COOH	H	*o*-OPh	24	7.3	
1j	$CONH_2$	H	*o*-OPh	9	7.0	
1k	COOH	H	*m*-SO_2CH_3	177	6.9	
1l	$CONH_2$	H	*m*-SO_2CH_3	>115	6.7	
1m	$CONH_2$	cyclopentyl	*o*-OCH_3	1	7.3	<5
1n	$CONH_2$	cyclopentyl	*o*-OH	6	7.3	5.4
1o	$CONH_2$	cyclopentyl	*o*-OisoPr		6.9	<5
1p	$CONH_2$	cyclopentyl	*o*-OPh	52	6.6	<5
1q	$CONH_2$	cyclopentyl	*o*-OCF_3	2	6.5	<5
1r	$CONH_2$	cyclopentyl	*o*-$N(CH_3)_2$	2	6.3	<5
1s	$CONH_2$	cyclopentyl	*o*-CH_2CN	96	6.1	
1t	$CONH_2$	cyclopentyl	*o*-CF_3	12	5.9	

[a] Solubility

A 2.4-Å resolution crystal structure was obtained of the kinase domain of CAMKK2 bound to **1b** using a construct with a deletion in the N-terminal domain necessary for crystallization (149-465, Δ205-220).[18] The assumed binding mode for the series was confirmed (Figure 2), including direct interaction between the ligand carboxylic acid and the catalytic lysine, Lys194. A

structured water molecule coordinated between the ligand, Lys194 and Asp330 may explain some initial SAR, as modeling suggests it may become frustrated in the presence of the *ortho*-substitued benzamide. The large gatekeeper residue Phe267 precludes penetration deeper into the so-called inner hydrophobic area. However, Leu269 at the edge of the hinge does provide an opportunity to improve selectivity. Close van der Waals contacts between the ligand and this residue can incur a steric bump and loss of potency against the >60% of kinases that boast a large residue (Phe, Tyr, Trp) at this position, a strategy that has been exploited elsewhere.[19]

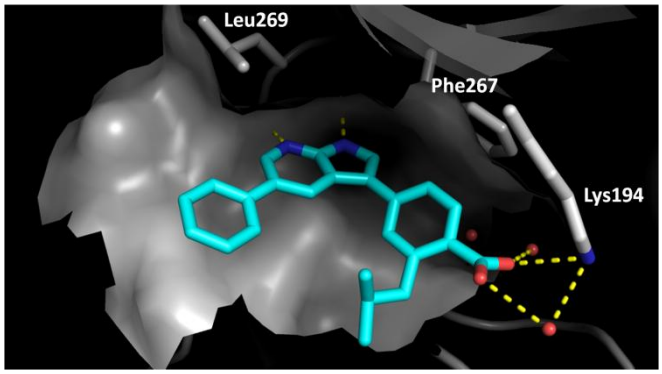

Figure 2. Crystal structure of CAMKK2 kinase domain deletion mutant bound to **1b.** Hydrogen bonds to ligand of ≤3 Å are shown. The N-terminal domain has been clipped and only a partial molecular surface is shown for clarity.[20]

Substitution at the *ortho*-position on the terminal phenyl could theoretically access the space near Leu269. However, despite modest potency improvements with small substitution independent of polarity (**1m**-**1t**), selectivity improvements were modest to nonexistent. We presumed that rotation about the biaryl bond allows the *ortho*-substituent to orient away from the hinge upon binding, thereby negating the intended effect on selectivity.

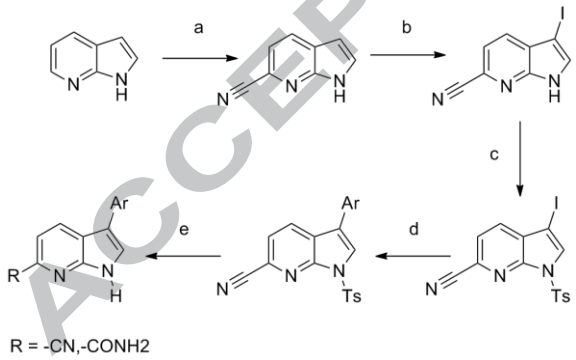

Scheme 2. Reagents and conditions: (a) 1.2 eq mCPBA, 2.5 eq Et_3N, 6 eq TMSCN in DCM under N_2, RT, 1 hr (b) 1 eq ICl in DCM, 20 °C, 1 hr, (c) 1.2 eq pTsCl, 0.02 eq Bu_4NBr, in 20:1 DCM:NaOH, 20°C, 1 hr, (d) 1.2 eq $ArB(OH)_2$, 0.05 eq $Pd(dppf)Cl_2$, 3 eq K_2CO_3 in 2.5:1 1,4-dioxane:water, 90 °C, 3 hr, (e) 1 eq NaOH in MeOH, 50 °C for 30 min (R=-CN) or 19 hrs (R=-$CONH_2$).

We therefore attempted to more directly access the space near Leu269 from the 6-position of the 7-azaindole, forgoing substitution at the 5-position (Table 2). A representative synthetic route is provided in Scheme 2. Our selectivity goals were realized with this substitution pattern: compound **2c** is inactive on all other kinases screened (>40 kinases with IC50 >10 μM, not shown), and as such, represents a remarkably compact and selective CAMKK2 inhibitor. Once again however, the benzoic acids showed poor cellular potency (**2b**-**2d**, **2f**) and the potency benefit of alkyl substitution is incompatible with the terminal amide (**2h-2j**).

We turned our attention to the pyrimidine series, hopeful that we could borrow SAR at several positions. Synthesis of 2-anilino, 4-aryl pyrimidines has also been described,[21] and conditions used here represent only minor deviations (Scheme 3). As expected, the unhindered benzoic acid and benzamide are again equipotent (**3a**-**3b** in Table 3). It is interesting that some kinases do not tolerate the acid as a lysine contact, perhaps because of a clash with the DFG aspartate, conserved glutamate on the C-helix, or intervening waters. For example, the amide is ~1000x more potent on CLK2 than the acid (data not shown). This observation serves as a reminder that profound selectivity between kinases can be obtained targeting perfectly conserved features.

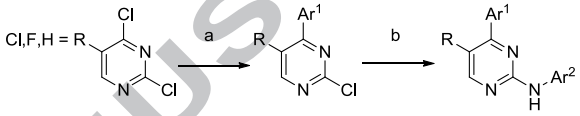

Scheme 3. Reagents and conditions: (a) 1 eq $Ar^1B(OH)_2$, 3eq $K_3PO_4.3H_2O$, 0.03 eq $Pd(PPh_3)_4$ in 4:1 1,4-dioxane: water, 80 °C, overnight, (b) 1 eq Ar^2NH_2, 1.2 eq K_2CO_3, 0.15 eq $Pd_2(dba)_3$, 0.15 eq BINAP in 1:1 1,4-dioxane:EtOH, 100 °C, overnight.

We attempted to implement our aforementioned selectivity strategy of targeting close contact with Leu269 by substituting at the *ortho*-position on the aniline (**3c**-**3e**). Unlike the 7-azaindole, bulk *ortho*- to the amine would sterically limit rotation of the aniline torsion and thereby maximize the desired effect on selectivity. Comparison of **3b** and **3e**, for example, reveals how intolerant some kinases are of this substitution pattern (potencies on GSK3β, JNK1, and PI3Kγ are shown as examples).

Table 2. 3,6-disubstituted, 7-azaindoles.

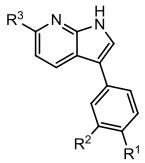

	R^1	R^2	R^3	Sol[a] (μM)	CAMKK2 pIC50	P-AMPK pIC50
2a	COOH	H	H		5.7	
2b	COOH	cyclopentyl	H	>290	8.5	5.4
2c	COOH	cyclopentyl	CN	155	7.8	5.2
2d	COOH	isopropyl	CN	>172	7.5	5.2
2e	COOH	H	CN	235	5.6	
2f	COOH	cyclopentyl	CH_3	>279	7.5	<5
2g	COOH	cyclopentyl	$CONH_2$	>205	5.9	
2h	$CONH_2$	H	H		6.4	
2i	$CONH_2$	cyclopentyl	CN	7	5.9	
2j	$CONH_2$	isopropyl	CN	14	5.5	

[a] Solubility

The abundance of aromatic rings makes it no surprise that solubility is a major developability hurdle for this series; not even the hydrophilic carboxylic acid can completely rescue the series' inherent poor solubility (**3a**). Truncation of the terminal phenyl resulted in a 10x loss in potency (**3f**), and did nothing to improve the solubility of the benzamide-containing analogs. Like the 7-azaindole series, the alkyl substitution adjacent to the amide did not significantly help potency, though it did restore some modicum of solubility (**3g**-**3h**), presumably disrupting packing in the solid phase. With minimal room between the ligand and the gatekeeper (Phe267), only conservative changes at the 5-position of the pyrimidine were attempted. Indeed, the modest potency benefit of the 5-fluoro substitution is lost with a larger halogen (**3h**-**3i**).

Table 3. 2-anilino, 4-aryl pyrimidines.

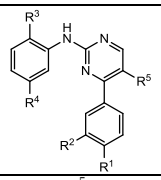

	R^1	R^2	R^3	R^4	R^5	Sol[a] (μM)	CAMKK2 pIC50	P-AMPK pIC50	GSK3β pIC50	JNK1 pIC50	PI3Kγ pIC50
3a	COOH	H	H	phenyl	H	14	8.1	5.1	6.4	6.4	7.9
3b	$CONH_2$	H	H	phenyl	H	3	8.1	6.2	7.5	6.0	7.0
3c	$CONH_2$	H	F	phenyl	H	3	7.7	5.1	5.6	<5	<5
3d	$CONH_2$	H	CH_3	phenyl	H	4	7.5	5.4	<4.6	<5	<5
3e	$CONH_2$	H	OCH_3	phenyl	H	7	7.9	<5	<4.6	<5	5.1
3f	$CONH_2$	H	OCH_3	H	H	<1	7.0	<5	<4.6	5.7	<5
3g	$CONH_2$	isopropyl	OCH_3	H	H	10	7.2	<5	<4.6	5.8	5.6
3h	$CONH_2$	isopropyl	OCH_3	H	F	11	7.4	5.5	5.1	5.5	<5
3i	$CONH_2$	isopropyl	OCH_3	H	Cl	5	6.8	<5	4.7	<5	5.2
3j	COOH	H	OCH_3	H	H	>444	6.7	<5	<4.6	5.3	5.4
3k	COOH	isopropyl	OCH_3	H	H	>367	8.7	6.0	4.8	5.5	5.8
3l	COOH	isopropyl	OCH_3	H	F	97	9.0	6.4	5.1	5.5	5.2

[a]Solubility

Truncation of the terminal phenyl did benefit the solubility of the acid containing analogs (**3j**-**3l**), and consistent with previous SAR, the addition of a branched alkane adjacent to the acid provided a strong potency improvement, again resulting in extremely efficient and selective, albeit unprogressable, CAMKK2 inhibitors (**3k**-**3l**).

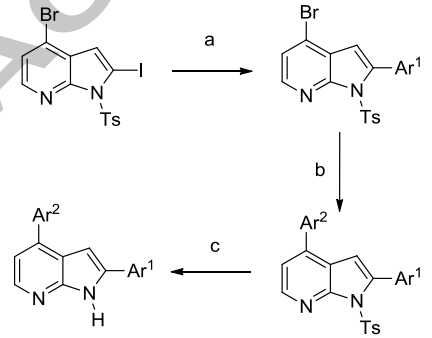

Scheme 4. Reagents and conditions: (a) 1 eq $Ar^1B(OH)_2$, 9.92 eq Na_2CO_3, 1.385 eq $Pd(PPh_3)_4$ in 1,4-dioxane, 120 °C, reflux, overnight, (b) 1 eq $Ar^2B(OH)_2$, 2 eq Na_2CO_3, 0.05 eq $PdCl_2$ (dppf)-CH_2Cl_2 adduct in 1,4-dioxane, 100 °C, 17 hrs, (c) 3 eq K_2CO_3, in MeOH, 50 °C, 4 hrs.

Neither series afforded truly potent inhibitors unless a carboxylic acid was present as the catalytic lysine contact. Low-dose pharmacokinetic (PK) properties of several acid-containing analogs were measured, and our assumptions about the limitations of these molecules were confirmed, revealing poor absorption from oral dosing and/or limited CNS exposure from IV dosing, with median brain concentrations typically < 10% of that seen in plasma. On the other hand, molecules such as **3h** did show CNS penetration with a > 1:1 brain to plasma ratio, however poor solubility precluded oral dosing.

Attempts to introduce solubilizing groups to the aniline of the pyrimidine-benzamide series did improve solubility in some cases where the terminal phenyl had been truncated (not shown), however, potency remained flat and limited progression. At the same time, our third hit (**4a**) had profoundly improved solubility due to its pendant cationic amine, and also hinted that single-digit nanomolar potencies could be achieved in the absence of a benzoic acid moiety. Molecule **4a** itself has an intrinsic clearance near hepatic blood flow when dosed in rats intravenously and is therefore insufficient as a tool. Screening of existing analogs in the corporate collection (**4b**-**4f**) plus additional chemistry efforts to expand SAR (**4g**-**4m**) revealed a much higher potency threshold than had been seen thus far, with potency not being exclusive to >10 μM solubility (Table 4). An established synthetic route[22] formed the basis for rapid analog creation (Scheme 4). Solubilizing groups at the solvent front are robustly tolerated at a variety of positions, but with little effect on potency. The combined improvements in potency and physical

properties within the series translated to cellular activities surpassing 100 nM.

Again, introduction of a branched alkane adjacent to the amide was equivocal on potency. While no head-to-head SAR was generated with regards to central exposure in this series, every *ortho*-alkyl benzamide tested had higher brain to plasma ratios over every unsubstituted benzamide tested (data not shown), encouraging us to continue to explore analogs with this substitution pattern. Indeed, compounds such as **4o** are approaching tool compound status with potent cellular activity and moderate clearance and CNS exposure, albeit with only modest $AUC_{0\text{-}6hr}$ when dosed orally (Table 5).

As we were now obtaining potencies better than 3 nM, we began to reconsider if a loss in potency could be tolerated for improved metabolic stability. The nitrile of **4q** and **4r** lost significant potency relative to their amide analogs, **4j** and **4l**, however, reintroduction of the *o*-isopropyl group restored much of the activity (**4s**-**4t**). Furthermore, there appeared to be some selectivity advantages to cyano substitution, eliminating all

Table 4. 2,4-diaryl 7-azaindoles.

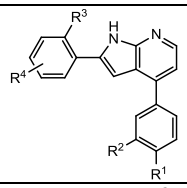

	R^1	R^2	R^3	R^4	Sol[a] (uM)	CAMKK2 pIC50	P-AMPK pIC50	IKK1 pIC50	JNK1 pIC50	INSR pIC50
4a	$CONH_2$	H	H	*p*-$CH_2N(CH_3)_2$	157	8.5	6.8	7.1	7.1	6.5
4b	$CONH_2$	H	H	*m*-$CH_2N(CH_3)_2$	56	8.4	6.9	7.1	6.2	6.2
4c	$CONH_2$	H	H	*p*-$CONH(CH_2)_3N(CH_3)_2$	29	8.8	<5	7.1	6.9	6.8
4d	$CONH_2$	H	H	*m*-$CONH(CH_2)_3N(CH_3)_2$		8.6	5.4	6.9	6.2	5.5
4e	$CONH_2$	H	H	*p*-$NHSO_2CH_3$	5	8.7	6.5	7.5	7.2	6.5
4f	$CONH_2$	H	H	*m*-$NHSO_2CH_3$	13	8.5	5.5	6.8	6.7	5.9
4g	$CONH_2$	H	OCH_3	H	16	8.5	6.1	6.8	6.8	5.8
4h	$CONH_2$	H	CH_3	3-CH_2-morpholine	18	8.8	6.7	7.0	6.5	5.9
4i	$CONH_2$	H	CH_3	4-CH_2-morpholine	18	8.1	5.7	6.9	6.2	5.4
4j	$CONH_2$	H	CH_3	5-CH_2-morpholine	2	8.8	7.5	5.5	5.2	<5
4k	$CONH_2$	H	CH_3	3-$O(CH_2)_2$-morpholine	17	8.7	6.6	6.8	6.6	5.5
4l	$CONH_2$	H	CH_3	4-$O(CH_2)_2$-morpholine	11	8.8	6.8	6.9	6.7	5.9
4m	$CONH_2$	H	CH_3	5-$O(CH_2)_2$-morpholine	17	8.7		6.7	6.8	5.4
4n	$CONH_2$	isopropyl	CH_3	5-CH_2-morpholine	1	8.8	6.7	6.8	6.2	<5
4o	$CONH_2$	isopropyl	CH_3	4-$O(CH_2)_2$-morpholine	4	9.1	7.2	5.6	5.7	6.4
4p	$CONH_2$	cyclopentyl	OCH_3	H	7	8.7	7.0	5.6	5.7	6.1
4q	CN	H	CH_3	5-CH_2-morpholine	2	7.1	5.6	<4.6	<5	<5
4r	CN	H	CH_3	4-$O(CH_2)_2$-morpholine	9	7	5.1	<4.5	4.7	<5
4s	CN	isopropyl	CH_3	5-CH_2-morpholine	1	7.9	6.4	5.6	5.1	<5
4t	CN	isopropyl	CH_3	4-$O(CH_2)_2$-morpholine	<1	8.2	6.3	<4.6	<5	<5

[a]Solubility

measureable activity on some kinases, such as INSR, Aurora A and DDR2 (IC50 > 10 μM), and significantly reducing potency on others, such as IKK1 and JNK1 (Table 4). Despite low aqueous solubility, molecule **4t** could be formulated for oral dosing and achieved our pharmacokinetic goals of reduced clearance, improved brain exposure (near 1:1 brain:plasma), and increased $AUC_{0\text{-}6hr}$ (nearly 8-fold) relative to its benzamide counterpart **4o** (Table 5).

We advanced **4t** into an acute efficacy study. Sprague Dawley rats were pretreated with a 30 mg/kg p.o. dose of **4t** or vehicle alone 2 hours before food was offered.[24] An hour after compound/vehicle dosing, animals were dosed i.c.v. with either 1 μM ghrelin or 3 μL saline. Food intake was monitored for 4 hours. Figure 3 shows the expected dramatic increase in cumulative food intake after 4 hours when ghrelin was administered in the absence of the CAMKK2 inhibitor (P = 1E-8), and a statistically significant 40% reduction of ghrelin-induced feeding in the presence of **4t** (P = 0.0004). Compound **4t** did not reduce feeding in the absence of ghrelin treatment, consistent with its mechanism of action.

Table 5. Pharmacokinetic properties of sample compounds.[23]

	Cl	$Dose_{p.o.}$ (mg/kg)	$AUC_{0\text{-}6hr,\ p.o.}$	$Cmax_{p.o.}$ (ng/ml)	B:P[a]
4o	50	30	572	374	0.6
4p	35	10	104	35	3.2
4s	30	30	1662	127	0.6
4t	24	30	4490	964	0.9

[a] Brain:Plasma ratio.

While we did not achieve all of our optimization goals in a single molecule, we believe that **4t** represents the first orally available, brain penetrant CAMKK2 inhibitor reported, and have demonstrated the pharmacological effect on satiety that was expected based on the building literature around CAMKK2's role in transducing ghrelin signaling in the hypothalamus. Furthermore, we present some profoundly selective compounds that may serve as *in vitro* tools or starting points for new optimization campaigns. As a final note, CAMKK1 activity was monitored throughout the optimization campaign and potency tracked CAMKK2 closely, so all molecules reported here should be treated as CAMKK1/2 dual inhibitors.[16]

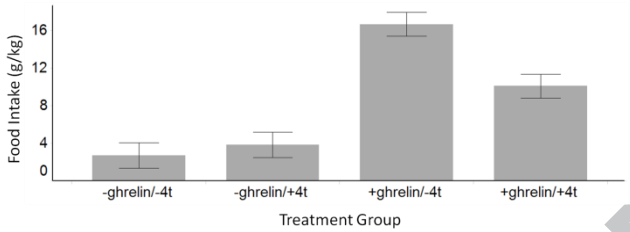

Figure 3. Cumulative grams of food intake per kilogram animal weight over 4 hours post ghrelin/saline treatment. Compound treated group contained 9 animals; vehicle treated 8 animals. Error bars reflect standard error of the mean based on pool standard deviation.

References and notes

1. Obesity: Preventing and Managing the Global Epidemic. WHO technical report series, 894. The World Health Organization, 2000.
2. Hardie, D.G., Ross, F.A., Hawley, S.A. *Nat. Rev. Mol. Cell. Biol.* **2012**, 13, 251.
3. Sakamoto, K., McCarthy, A., Smith, D., Green, K.A., Hardie, G., Ashworth, A., Alessi, D.R. *EMBO J.* **2005**, 24, 1810.
4. Shaw, R.J., Kosmatka, M., Bardeesy, N., Hurley, R.L., Witters, L.A., DePhino, R.A., Cantley, L.C. *Proc. Natl. Acad. Sci. USA*. **2004**, 101, 3329.
5. Anderson, K.A., Ribar, T.J., Lin, F., Noeldner, P.K., Green, M.F., Muehlbauer, M.J., Witters, L.A., Kemp, B.E., Means, A.R. *Cell Metab.* **2008**, 7, 377.
6. Anderson, K.A., Lin, F., Ribar, T.J., Stevens, R.D., Muehlbauer, M.J., Newgard, C.B., Means, A.R. *Mol. Endocrinol.* **2012**, 26, 281.
7. Cary, R.L., Waddell, S., Racioppi, L., Long, F., Novack, D.V., Voor, M.J., Sankar, U. *J. Bone Miner. Res.* **2013**, 28, 1599.
8. Peters, M., Mizuno, K., Ris, L., Angelo, M., Godaux, E., Giese, K.P. *J. Neurosci.* **2003**, 23, 9752.
9. Using black 384-well plates at RT, 0.1 μL of compound in DMSO solution was preincubated with 5 μL of enzyme solution (40 mM HEPES, pH 7.2, 1 mM CHAPS, 1 mM DTT, 1 mM $CaCl_2$, 4 nM full-length hCAMKK2, 1 μM hCalmodulin) for 30 min, followed by incubation with 5 μL substrate mixture (40 mM HEPES pH 7.2, 1 mM CHAPS, 1 mM DTT, 10 mM MgCl2, 20 μM ATP, 100 nM 5FAM-AKPKGNKDYHLQTCCGSLAYRRR-amide, 1 mM $CaCl_2$, 1 μM hCalmodulin) for 120 min before addition of 10 μL of 1:500 dilution IMAP bead solution for 60-90 min and read-out in fluorescent polarization mode with excitation at 485 nM and emission at 530 nM using a 505 nM dichroic lense.
10. 100 μL of resuspended N39 cells were dispensed into 96-well tissue culture plates (~1000 cells/well) and incubated overnight at 37°C and 5% CO2. 11 μL of compound in DMSO was then incubated with cells for 80 min, followed by treatment with 12 μL of 100 mM ionomycin. Media was removed, and cells were incubated with a Cell Extraction Buffer for 30 min on ice before dilution with ice-cold MSD lysis buffer containing protease and phosphatase inhibitors. Detection used a commercially available AMPKα pT172 Immunoassay Kit supplied by Invitrogen #KHO0651.
11. Mouse and rat CAMKK2 are >99% identical in the kinase domain, and identical in the ATP binding site (within 7 Å of ligand).
12. Aronov, A.M. Murcko, M.A. *J. Med. Chem.* **2004**, 47, 5616.
13. Young, R.J., Green, D.V.S., Luscombe, C.N., Hill, A.P. *Drug Discov. Today.* **2011**, 16, 822.
14. 5 μL of a 10 mM stock solution of compound in DMSO was diluted to 100 μL with a 10 mM phosphate buffered saline, pH 7.4, equilibrated for 1 h at RT, and filtered through Millipore MultiscreenHTS-PCF filter plates (MSSL BPC). The eluent was quantified by suitably calibrated flow injection Chemi-Luminescence Nitrogen Detection (CLND). See Reference 13.
15. Pajouhesh, H., Lenz, G.R. *NeuroRx.* **2005**, 2, 541.
16. CAMKK1 activities and some calculated and measured properties included in supplementary information.
17. Hong, S., Kim, J., Seo, J.H., Jung, K.H., Hong, S. Hong, S. *J. Med. Chem.* **2012**, 55, 5337.
18. PDB code: 6CMJ; see Supplementary Information for details of crystallography. Additionally, a crystal structure of 1a bound to CAMKK2B has recently been released by the Structural Genomics Consortium (pdb code: 6BKU), but at this time is unpublished.

19. Kothe, M., Kohls, D., Low, S., Coli, R., Rennie, G.R., Feru, F., Kuhn, C., Ding, Y. *Chem. Biol. Drug. Des*. **2007**, 70, 540.
20. Image generated with The PyMol Molecular Graphics System, Version 1.6.0.0 Schrödinger, LLC.
21. Xu, Y., Foulks, J.M., Clifford, A., Brenning, B., Lai, S., Luo, B., Parnell, K.M., Merx, S., McCullar, M.V., Kanner, S.B., Ho, K. *Bioorg. Med. Chem. Lett.* **2013**, 23, 4072.
22. Adams, N.D., Adams, J.L., Burgess, J.L., Chaudhari, A.M., Copeland, R.A., Donatelli, C.A., Drewry, D.H., Fisher, K.E., Hamajima, T., Hardwicke, M.A., Huffman, W.F., Koretke-Brown, K.K., Lai, Z.V., McDonald, O.B., Nakamura, H., Newlander, K.A., Oleykowski, C.A., Parrish, C.A., Patrick, D.R., Plant, R., Sarpong, M., Sasaki, K., Schmidt, S.J., Silva, D.J., Sutton, D., Tang, J., Thompson, C.S., Tummino, P.J., Wang, J.C., Xiang, H., Yang, J., Dhanak, D. *J. Med. Chem.* **2010**, 53, 3973.
23. 3 mg/kg i.v. dose. Compound formulated in 5% DMSO, 10% solutol®, and 85% saline. Reported parameters are averages from two male CD rats for each dosing group.
24. All studies were conducted in accordance with the GSK Policy on the Care, Welfare and Treatment of Laboratory Animals and were reviewed by the Institutional Animal Care and Use Committee either at GSK or by the ethical review process at the institution where the work was performed.
25. David H. Drewry: University of North Carolina, Structural Genomics Consortium, Center for Chemical Biology, Chapel Hill, NC 27599, USA. Brian D. Thompson: Exela Pharma Sciences, 1245 Blowing Rock Blvd., Lenoir, NC 28645. Paul R. Reid: US Army Research Office, 800 Park Offices Dr., Durham, NC, 27703. Patrick R. Maloney: Sanford Burnham Prebys Medical Discovery Institute, 6400 Sanger Rd., Orlando, FL 32827 . Xi Liang: MDDX Research & Informatics, 580 California St. Floor 16, San Francisco, CA, 94104. Paula K. Selley: Seattle Genetics, 21823 30th Drve S.E., Bothell, WA 98021. Octerlony B. McDonald: Retired . Jeffery L. Smith: No affiliation. Richard Cox: Kerr Health LTC, 8411 Garvey Dr., Raleigh, NC, 27616. Todd W. Shearer: Nuventra Pharma Sciences, 2525 Meridian Parkway, Suite 200, Durham, NC 27713. Stefano Tacconi, Federico Faggioni, Ilaria Sartori, and Michela Tessari: Aptuit Center for Drug Discovery and Development, 37135 Verona, Italy. Chiara Piubelli: Laboratory of Molecular Biology, Centre for Tropical Diseases, Sacro Cuore-Don Calabria Hospital, Via Don A. Sempreboni, 5-37024 Negrar-Verona. Tony Wang: Kunming Biomed International, No. 1 Boda Rd. Yuhua District, Chenggong New Town, Kunming, P.R. China 650600.

Graphical Abstract

An orally available, brain-penetrant CAMKK2 inhibitor reduces food intake in rodent model

Leave this area blank for abstract info.

Daniel J. Price, David H. Drewry, Lee T. Schaller, Brian D. Thompson, Paul R. Reid, Patrick R. Maloney, Xi Liang, Pierette Banker, Richard G. Buckholz, Paula K. Selley, Octerloney B. McDonald, Jeffery L. Smith, Todd W. Shearer, Richard Cox, Shawn Williams, Robert A. Reid, Stefano Tacconi, Federico Faggioni, Chiara Piubelli, Ilaria Sartori, Michela Tessari, and Tony Y. Wang

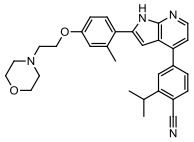

4t
CAMKK2 pIC50 = 8.2
P-AMPK pIC50 = 6.3
B:P = 0.9